## Conclusion

The structure of a pseudo-rhombohedral polymorph of $Cu_2ZnGeS_4$ has been determined by a combination of lattice imaging and convergent-beam and selected-area electron diffraction.

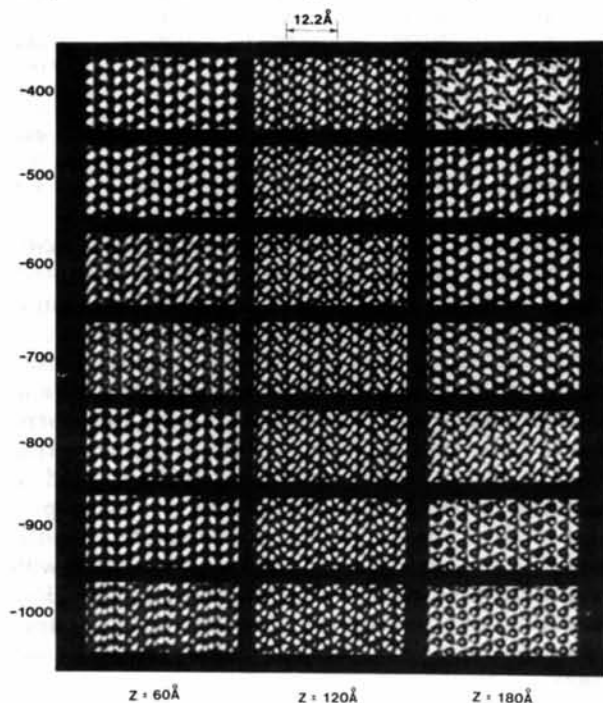The unusual stacking sequence *hhcc* of this polymorph was determined by direct interpretation of



Fig. 18. Multislice calculations using $C_s$ of 0·94 mm of the refined *hhcc* $Cu_2ZnGeS_4$ structure viewed down the *c* axis with 200 kV electrons. Calculations are presented for seven defects of focus (Å) as indicated at the left of the diagram for each of three thicknesses $z=60$, 120 and 180 Å as indicated at the bottom of the diagram.

lattice images obtained with 200 kV electrons. The intensity distribution of the sublattice reflections of electron diffraction patterns of crystals in several orientations confirmed the outline structure. The ordering of cations was determined, and initial refinement of S-atom positions was achieved, from details of the superlattice, such as dark bands on some CBED discs and the absence or presence of other reflections.

Various dynamical effects, most obviously the breakdown of Friedel's law, were found to be decisive aids at various stages in the determination of the structure; for instance the unequivocal assignment of the space groups.

A second polymorph of $Cu_2ZnGeS4$ was shown by CBED to have the same ordering in cubic stacking and thus to be tetragonal and isostructural with stannite $Cu_2FeSnS_4$.

### References

AMELINCKX, S. (1979). *Dislocations in Solids.* Vol. 2, ch. 6, edited by F. R. N. NABARRO. Amsterdam: North-Holland.
BROCKWAY, L. O. (1934). *Z. Kristallogr.* **89**, 434–441.
HAUSSUEHL, S. & MUELLER, G. (1963). *Beitr. Mineral. Petrogr.* **9**, 28–33. (*Chem. Abstr.* **59**: 4905d.)
MOH, G. H. & OTTEMAN, J. (1962). *Neues Jahrb. Mineral Abh.* **99**, 1–28
MOODIE, A. F. & WHITFIELD, H. J. (1983). *Acta Cryst.* A**30**, 946–947.
MOODIE, A. F. & WHITFIELD, H. J. (1984). *Ultramicroscopy,* **13**, 265–278.
OLSEN, A. & SPENCE, J. C. H. (1981). *Philos. Mag.* **43**, 945–965.
PARTHÉ, E. (1972). *Cristallochimie des Structures Tetraédriques.* New York, London: Gordon and Breach.
PAULING, L. & HUGGINS, M. L. (1934). *Z. Kristallogr.* **87**, 205–238.
RAMDOHR, P. (1944). *Abh. Preuss, Akad. Wiss.* **4**, No. 4. (*Chem. Abstr.* **40**: 6023⁹.)
SAYRE, D. (1951). *Acta Cryst.* **4**, 60–65.
SPENCE, J. C. H. (1983). *Ultramicroscopy,* **11**, 117–124.

# Electron Charge Density and Electron Momentum Distribution in Magnesium Oxide

By M. Causà', R. Dovesi, C. Pisani and C. Roetti

*Institute of Theoretical Chemistry, University of Turin, Via P. Giuria 5, I-10125 Torino, Italy*

## Abstract

The electronic structure of magnesium oxide is presented and discussed, as resulting from a LCAO crystalline-orbital Hartree–Fock extended-basis-set computation. Mulliken populations, charge density maps, structure factors, electron momentum distribution and Compton profiles are provided. They are compared with the results of simple theoretical models, and with available experimental data. The present study confirms the fully ionic character of MgO; it also shows that there is a certain anisotropy of the oxygen ion in the crystalline environment, and that the magnesium ion is slightly expanded with respect

to the free-ion solution. The agreement with experimental data is on the whole satisfactory, but it appears that more reliable measurements of structure factors are needed in order to assess the accuracy of the present results.

## Introduction

It is generally assumed that the electronic structure of magnesium oxide is adequately described by the configuration $Mg^{2+}O^{2-}$, where the ion $O^{2-}$ is stabilized by the crystalline field. In a comparative study of electron charge distributions in MgO, CaO, SrO, BaO, as resulting from X-ray scattering data, Vidal-Valat, Vidal & Kurki-Suonio (1978) have, however, come to the conclusion that ionicity increases along the series, and that the distribution of electrons around the magnesium cation in MgO corresponds more closely to $Mg^+$ than to $Mg^{2+}$. On the other hand, Compton profile data (Berggren, Manninen, Paakkari, Aikala & Mansikka, 1977; Aikala, Paakkari & Manninen, 1982), which are more sensitive to the distribution of valence electrons, give results that favour the fully ionic structure. In both cases, accurate calculations for MgO could help us to discriminate between different possibilities and to analyse experimental data.

In the present work, we describe the electron distribution in magnesium oxide as resulting from an *ab initio* all-electron crystalline-orbital LCAO Hartree-Fock treatment (Pisani & Dovesi, 1980; Dovesi, Pisani, Roetti & Saunders, 1983). Details of the computation have been given in a previous paper (Causa', Dovesi, Pisani & Roetti, 1986) whose main object is to compare the stable 'NaCl' phase of MgO with two hypothetical crystal structures, 'CsCl' and (inverse) 'NiAs'; we recall here that a moderately extended basis set comprising three *s* orbitals and six *p* orbitals per atomic species has been used; the parameters defining the shape and size of the atomic orbitals have been variationally optimized: as a result, the calculated cohesive energy is fully compatible with experiment, after taking a reasonable estimate of the correlation contributions to energy. The same computational procedure has been used in past years to determine the electronic structure of a number of crystalline systems; among them, the ionic lithium compounds LiH (Dovesi, Ermondi, Ferrero, Pisani & Roetti, 1984), $Li_2O$ (Dovesi, 1985), $Li_3N$ (Dovesi, Pisani, Ricca, Roetti & Saunders, 1984). Because of the variational character of our study and of the use of an extended basis set, we believe that the essential features of the electron distribution, first of all electron transfer and ion deformation, are correctly described.

The results are presented in the following according to different viewpoints. Mulliken populations are first given and critically analysed: they provide valuable

Table 1. *Contribution to the Mulliken populations of the different species of atomic orbitals from the different occupied bands*

| | Magnesium | | Oxygen | |
| Band | s | p | s | p |
|---|---|---|---|---|
| 1 | 2·000 | 0·000 | 0·000 | 0·000 |
| 2 | 0·000 | 0·000 | 2·000 | 0·000 |
| 3 | 1·999 | 0·000 | 0·001 | 0·000 |
| 4 | 0·000 | 1·991 | 0·005 | 0·004 |
| 5 | 0·000 | 1·996 | 0·000 | 0·004 |
| 6 | 0·000 | 1·998 | 0·000 | 0·002 |
| 7 | 0·001 | 0·008 | 1·985 | 0·006 |
| 8 | 0·003 | 0·008 | 0·012 | 1·977 |
| 9 | 0·000 | 0·011 | 0·001 | 1·988 |
| 10 | 0·001 | 0·005 | 0·000 | 1·994 |
| Total charge | 4·004 | 6·017 | 4·004 | 5·975 |

though indirect information on the degree of ionicity. The electron charge distribution is then presented: on the one hand, comparison is effected with simple models that consider the superposition of atomic or ionic distributions, by providing difference density maps which show evidence of charge transfer and ion deformation effects; on the other hand, the experimental information available from X-ray scattering studies (Sanger, 1969; Lawrence, 1973) is used to calculate Debye-Waller factors and to discuss possible inadequacies of the calculated results. Finally, the electron momentum distribution is described, with special attention given to anisotropy effects; the calculated Compton profiles are compared with the ones obtained from γ-ray measurements (Aikala *et al.*, 1982).

## Results and discussion

Table 1 reports the Mulliken populations corresponding to the different occupied bands and to the different types of atomic orbitals (*s* or *p*) on magnesium and oxygen. It is known that the Mulliken partition scheme can be criticized from two points of view: (i) the off-diagonal terms $P_{\mu\nu}S_{\mu\nu}$ are attributed half to each of the involved atomic orbitals, whereas the corresponding charge distribution $P_{\mu\nu}\chi_\mu(\mathbf{r})\chi_\nu(\mathbf{r})$ is nearer to the less-diffuse one; the 'error' can be particularly large in the case of core-valence terms; in the present case, however, the overlap populations are so small ($-0·011$, $-0·012$ and $0·000$ electrons for the first-neighbour magnesium-oxygen, oxygen-oxygen and magnesium-magnesium atoms respectively) that their partition is not critical at all; (ii) when large basis sets including very diffuse functions are used, the Mulliken populations can be altered at will; in fact in this case the AO's centred on a given atom contribute to the description of many other atoms and relatively similar charge distributions can give quite different Mulliken charges. This is, however, not the case in our calculation, where a moderately extended basis set of essentially localized atomic orbitals has been employed (the exponent of

the outer Gaussian is 0·4 and 0·21 a.u. for magnesium and oxygen, respectively). In the present case Mulliken population data can then be used with some confidence.

The Mulliken analysis of Table 1 confirms the completely ionic character of magnesium oxide, since the excess population on magnesium with respect to the $Mg^{2+}$ configuration is only 0·021 electrons. Also, it can be noticed that all occupied bands can unambiguously be classified as belonging to either oxygen or magnesium; this will prove useful in the following, when correcting the theoretical structure factors in order to account for thermal motion.

The Mulliken populations of the different orbitals can also be used to verify the deformation of the cation in the crystalline field. It is in particular interesting to see how the electrons of the $L$ shell of magnesium are distributed among the two sets of orbitals that have been associated with that shell: an internal $sp$ set, which describes the electrons in the proximity of the core, and an outer one corresponding to a single Gaussian with exponent coefficient 0·40 a.u. In the isolated ion, the outer orbitals are practically not populated; in the crystal environment, the populations on the two orbital sets are 1·999, 0·006 for $s$ electrons, and 1·996, 0·010 for $p$ electrons, respectively. There is therefore a small but not negligible expansion of the magnesium core, associated with a gain in crystal energy of about 0·01 eV. It can finally be mentioned that the Mulliken partition scheme is also utilized for the evaluation of the atomic multipoles. In the present case, owing to the symmetry, the first non-zero multipoles are the hexadecapole $\gamma_4^0$ ones [see, for example, Dovesi et al. (1983) for the definition]. Their value is 0·0284 and −2·510 a.u. for magnesium and oxygen, respectively. As expected, the anions are much more anisotropic than the cations; oxygen appears to be slightly compressed in the direction of the neighbouring magnesium ions, probably because of orthogonality constraints, while the reverse is true for magnesium.

By contrast with Mulliken populations, the electron density $\rho(r)$ is a well defined physical quantity, but does not lend itself to providing unambiguous numerical parameters related to bond populations, charge transfer and the like. For instance, using the total charge contained within a sphere as a measure of ionicity [as done for instance by Vidal-Valat et al. (1978)] may be criticized on the grounds that minima in electron density are difficult to identify, and that it is implicitly assumed that charge distributions are isotropic around the cores. It is perhaps more informative to make reference to relatively rough models, which have however a clear physical meaning. Difference density maps can be used for this purpose: they immediately show how far and in which way the calculated distribution differs from the model density.

Fig. 1 shows difference (calculated minus model) density maps, referring to different model charge distributions, obtained by superposing the contributions from individual atoms or ions. For neutral magnesium and oxygen (Fig. 1a) the Hartree–Fock atomic wavefunctions were used. In the two other cases, an ionic model has been assumed and the Hartree–Fock solution has been used for the $Mg^{2+}$ ion. As regards the $O^{2-}$ ion, in Fig. 1(b) it has been described according to the Watson (+2 well) model (Watson, 1958), corresponding to the Hartree–Fock solution for an isolated oxygen ion, stabilized by a sphere of +2 charge. In Fig. 1(c), the Yamashita model has been used (Tokonami, 1965; Yamashita &
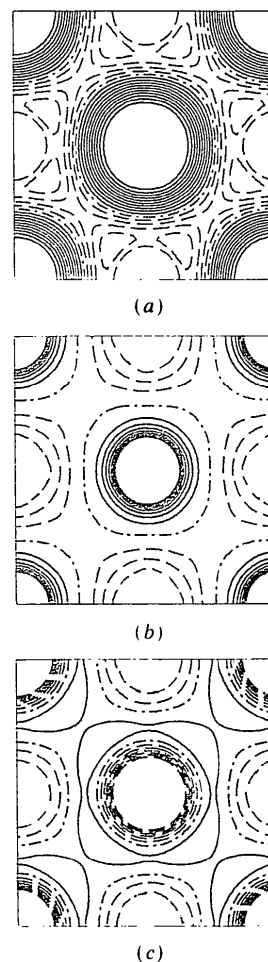


(a)

(b)

(c)

Fig. 1. Difference charge density maps (calculated minus model density), for three types of superposition models: (a) Hartree–Fock atoms; (b) Watson (+2 well) model (Watson, 1958); (c) Yamashita model (Yamashita & Asano, 1970). The oxygen atoms are at the centre and at the corners of each plot, the magnesium atoms at the midpoint of the sides of the square. Each curve corresponds to a given level of difference density: continuous lines correspond to positive, dashed lines to negative difference density; the zero lines are the dot-dashed ones; the distance between two consecutive curves is 0·0025 a.u. (1 a.u. = 6·7487 electron $Å^{-3}$).

Asano, 1970): here, $s$ electrons are described according to the Watson (+1 well) model, while the $2p$ functions are determined using a Green-function technique. The choice of the latter two models is due to the fact that they give a simple but quite reasonable description of the $O^{2-}$ ion as stabilized by the crystalline field (the Yamashita model also includes exchange interactions with the magnesium ions), and that they have often been used with remarkable success in the discussion of experimental data (Burley, 1965; Togawa, 1965; Raccah & Arnott, 1967; Dawson, 1969; Sanger, 1969; Togawa, Inkinen & Manninen, 1971; Berggren et al., 1977; Aikala et al., 1982). It is apparent from Fig. 1(a) that there is an important build-up of electron charge around oxygen with respect to the atomic superposition model. The other two plots show that the present results are very similar to those obtained with the fully ionic models, except in the oxygen core regions. To be more precise, it can be noticed that the Yamashita model describes the oxygen ion as slightly more compressed than resulting from the present investigation, while the reverse happens with the Watson model. Incidentally, using the Watson (+1 well) model leads to results that are indistinguishable from those of the +2 well model in the scale of the figure. As regards the magnesium ion, Figs. 1(b) and 1(c) show that in the crystalline field it experiences a slight expansion with respect to the free-ion solution. The picture emerging from the Mulliken population analysis is therefore fully confirmed.

The quality of the calculated $\rho(\mathbf{r})$ can in principle be assessed by comparing theoretical with experimental structure factors. Such a test is however rather indirect, in view of the number of assumptions and corrective terms that are needed. This has been clearly demonstrated by Dawson (1969) in a critical review of work concerning (among others) structure factors of magnesium oxide: a subtle analysis is needed for a correct refinement of intensity data, prior to ascertaining the superiority of one or other theoretical model or to recognizing the poor quality of an experimental set. In the present case we are in a sense in a favourable position because we can evaluate the static structure factors by performing a direct Fourier transform of the whole $\rho(\mathbf{r})$, so preserving anisotropic terms associated with ion–ion interaction. However, some kind of partition is needed if we want to include corrections for zero point and thermal motion which are different for the different ions. We have proceeded as follows. The static structure factors have been calculated for the individual occupied bands; the factors for the two species have then been obtained by summing the contributions from the respective bands (1, 3, 4, 5, 6 for magnesium, 2, 7, 8, 9, 10 for oxygen). For comparison with the experimental data, allowance was made for independent isotropic Debye–Waller factors for oxygen and magnesium, and for the real part $f'$ of the anomalous-dispersion

Table 2. *Debye–Waller factors for magnesium oxide in* $\text{Å}^2$

The average $B$ factor is defined as $\tilde{B} = (m_{\text{Mg}}B_{\text{Mg}} + m_{\text{O}}B_{\text{O}})/(m_{\text{Mg}} + m_{\text{O}})$.

| Determination | $B_{\text{Mg}}$ | $B_{\text{O}}$ | $\tilde{B}$ |
|---|---|---|---|
| Present: best fit with Sanger (1969) X-ray data | 0·341 | 0·312 | 0·330 |
| Present: best fit with Lawrence (1973) X-ray data | 0·336 | 0·336 | 0·336 |
| Togawa (1965): best fit with his own X-ray data, using Tokonami (1965) model for $O^{2-}$ | 0·24 | 0·19 | 0·22 |
| Sanger (1969): best fit with his own X-ray data, using Watson (+2 well) model for $O^{2-}$ (Watson, 1958) | 0·346 | 0·315 | 0·334 |
| Lawrence (1973): best fit with his own X-ray data, using atomic scattering factors | 0·31 | 0·34 | 0·32 |
| Beg (1976): best fit with his own neutron scattering data | — | — | 0·354 |
| Gupta & Haridasan (1973): dynamical calculation | 0·30 | 0·33 | 0·31 |
| Barron (1977): thermodynamic determination | — | — | 0·3085(300) |

correction (Sanger, 1969). This procedure is questionable in principle, but seems well founded here on two grounds: firstly, the attribution of the different bands to the two species is justified on the basis of the Mulliken analysis; secondly, the thermal factors for oxygen and magnesium turn out to be very similar, so the partition is far from critical.

The procedure described has been applied with reference to the single-crystal X-ray data produced by Sanger (1969) and by Lawrence (1973). Sanger used a sample which had been neutron irradiated in order to overcome the effects of extinction. His measured structure factors, whose accuracy was estimated to be about 2%, encompass a much wider range of reflections (from 111 to 666) than in previous investigations (Burley, 1965; Togawa, 1965; Raccah & Arnott, 1967). Sanger's data have been used in the paper by Vidal-Valat et al. (1978) for comparing the charge distribution of MgO with that of other alkaline earth oxides. Lawrence used an undamaged single crystal and considered high-angle reflections only, with the primary purpose of accurately determining the Debye–Waller factors. The Debye–Waller factors obtained by best fit with the two experimental sets are reported in Table 2 along with other determinations, both from theoretical calculations (Gupta & Haridasan, 1973) and from independent experimental data (Beg, 1976; Barron, 1977). Apart from the Togawa determination, which is clearly anomalous, and the Beg results from neutron diffraction measurements, which are slightly too high, all other determinations are reasonably close to each other; in the following we shall use the factors obtained by best fit with Lawrence's data which are the most reliable ones according to Barron's (1977) comprehensive discussion.

For all reflections considered by Sanger and/or by Lawrence, Table 3* reports the calculated structure factors for magnesium and oxygen, and the resulting MgO structure factors at room temperature. The agreement factor between present results and Lawrence's data is 0·0073. It is much worse with Sanger's data (0·0176), but improves to 0·0147 if the corresponding best-fit thermal factors are used (see Table 2); the latter agreement factor is practically the same as obtained when trying to fit the data by Sanger using the Yamashita or the Watson model for the oxygen ion. The reason for these results is clarified in Fig. 2. The data reported there refer to different determinations of the structure factors for oxygen at zero temperature. The theoretical factors corresponding to the Yamashita model (Tokonami, 1965) or to the Watson (+2 well) model (Watson, 1958) are directly compared with the present ones (third column in Table 3) in Fig. 2(a). It is seen that our results are intermediate between the two models, so confirming the observations referring to Fig. 1; on the whole, however, the three theoretical determinations are similar except for the first few reflections. The 'experimental' oxygen factors at zero temperature were obtained by subtracting from the observed intensities the theoretical contribution from the magnesium ion (which is essentially the same for all models) and by dividing the result by the corresponding Debye–Waller correction for oxygen; in Fig. 2(b) the oxygen structure factors obtained from Sanger's data according to such a procedure are compared with those of Lawrence and with the present ones. It is seen that the two experimental descriptions of the

oxygen ion are appreciably different from each other; the agreement between the two is only slightly better than the agreement between Sanger's and present data. This is not too surprising since the declared accuracy of Sanger's data is about 2%, which is comparable with the agreement factors obtained here. In summary, the present analysis shows that the available sets of structure factors are not able to discriminate between different current models of magnesium oxide: for this purpose, new accurate measurements of the first few structure factors would be needed on an absolute scale and referring to an undamaged crystal. As things are, a subtle analysis of the reconstructed charge density, such as that proposed by Vidal-Valat et al. (1978) starting from Sanger's data, is likely to lead to wrong conclusions.

Fig. 3 describes the distribution of electron momenta by providing the average density $\bar{\rho}(p)$ (top plot) and the anisotropies $\Delta\rho_{(hkl)}(p) = \rho_{(hkl)}(p) - \bar{\rho}(p)$ along the three main crystallographic directions (bottom plot). The anisotropy, though not negligible, is quite small, confirming the nearly spherical shape of the electron distribution around the ions. In the case of the lithium compounds previously considered (LiH, $Li_2O$, $Li_3N$), the anisotropy was larger, probably because of the stronger repulsion between the anions, favoured by the small dimension of $Li^+$. An analysis of the contributions from the different bands shows, as expected, that the anisotropy is almost entirely attributable to valence electrons.

In a recent paper Podloucky & Redinger (1984) reported electron momentum distribution (EMD) and Compton profile curves for MgO as obtained by an augmented-plane-waves calculation. Unfortunately the data are not tabulated, so that a point-to-point comparison is impossible; nevertheless, the essential features in the three directions are very similar to the present ones: the [111] curve is intermediate between the other two; the peak in the [100] direction is the broadest, and is shifted to higher

---

* Table 3, listing calculated structure factors for magnesium, oxygen and magnesium oxide, has been deposited with the British Library Lending Division as Supplementary Publication No. SUP 42680 (2 pp.). Copies may be obtained through The Executive Secretary, International Union of Crystallography, 5 Abbey Square, Chester CH1 2HU, England.
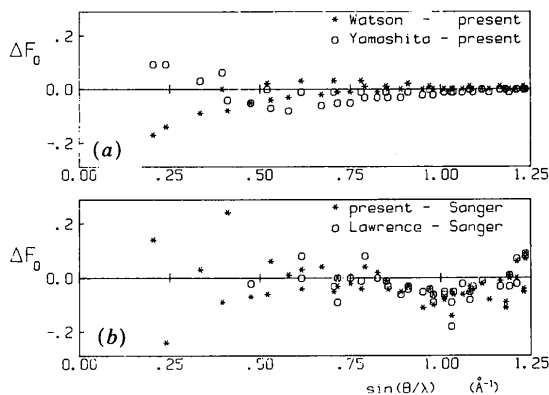


Fig. 2. Difference between various determinations of the static structure factors $F_O$ for the oxygen ion in magnesium oxide. For further explanations see text.
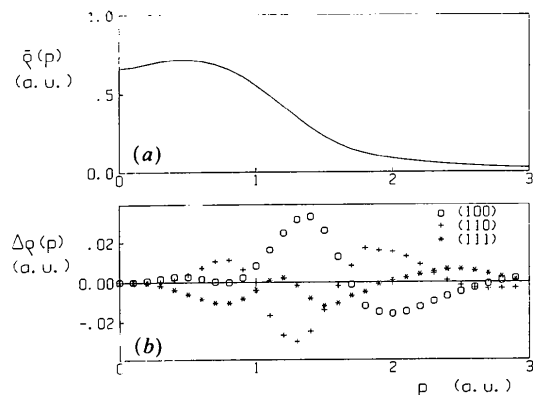


Fig. 3. Calculated electron momentum distribution (EMD) in magnesium oxide. (a) Average EMD, $\bar{\rho}(p)$; (b) EMD anisotropies $\Delta\rho_{(hkl)}(p) = \rho_{(hkl)}(p) - \bar{\rho}(p)$.

momenta; secondary peaks are found at 1·9, 2·2 and 2·9 a.u. in the [111], [110] and [100] directions, respectively, to be compared with 1·8, 2·5 and 3·1 a.u. obtained in the present calculation.

Experimental information on the EMD can be obtained by Compton profiles (CP). Whereas available X-ray data (Weiss, 1970; Togawa et al., 1971) are quite unreliable because of the fact that with X-rays multiple scattering events are important, and the impulse approximation fails for 1s electrons, useful information is provided by more recent $\gamma$-ray measurements (Berggren et al., 1977; Aikala et al., 1982). The experimental $\gamma$-ray CP's have been compared by these authors with theoretical curves obtained by orthogonalizing different kinds of ionic wave functions. Although none of the proposed models faithfully reproduces the most recent experimental results (Aikala et al., 1982) within the declared statistical error, nevertheless this analysis confirms the totally ionic character of MgO.

The results obtained with our variational approach are reported in Table 4, along with the isotropic Aikala profile. The agreement between the calculated and the experimental curves is satisfactory in the whole range of electron momenta; however, in the zero to 2 a.u. interval the disagreement is two to three times larger than the reported experimental statistical error. Apparently, the density of slow electrons ($0 < q < 0.5$ a.u.) is underestimated in the present calculation; this might indicate that there is some defect in the description of electrons in the interionic cavities, owing to basis-set limitations rather than to neglect of correlation terms: in fact the inclusion of the latter should increase the average electron momentum. On the other hand, residual experimental errors could be at the origin of the difference; in this respect it must be noticed that at low momenta Aikala's curve is appreciably lower (and nearer to ours) than the less-recent one (Berggren et al., 1977). A deeper comparison with the experimental data, and with the theoretical results of Podloucky & Redinger (1984), including an analysis of the anisotropy, of the autocorrelation function (Schülke, 1977; Pattison & Williams, 1976), and of basis-set effects would require much more space and is deferred to another paper.

## Concluding remarks

In contrast with the conclusions of Vidal-Valat et al. (1978), the present study strongly supports the idea of practically complete ionicity of magnesium oxide. This picture could, however, be changed to a greater or lesser extent when surfaces are considered, since the stabilization of the $O^{2-}$ ion by the crystalline field is less effective there. Apart from this major conclusion, the following comments can be put forward. In the crystalline environment the magnesium ion is slightly expanded with respect to the free-ion sol-

Table 4. *Directional and average Compton profiles of magnesium oxide*

$J_{(100)}$, $J_{(110)}$, $J_{(111)}$ are the calculated directional profiles. $\bar{J}_{HF}$ and $\bar{J}_\gamma$ are the average calculated and the isotropic experimental (Aikala et al., 1982) profiles, respectively. All quantities are in atomic units.

| $p$ | $J_{(100)}$ | $J_{(110)}$ | $J_{(111)}$ | $\bar{J}_{HF}$ | $\bar{J}_\gamma$ |
|---|---|---|---|---|---|
| 0·0 | 5·735 | 5·726 | 5·720 | 5·726 | 5·774(25) |
| 0·1 | 5·693 | 5·673 | 5·707 | 5·688 | 5·751 |
| 0·2 | 5·648 | 5·620 | 5·648 | 5·635 | 5·676 |
| 0·3 | 5·511 | 5·538 | 5·542 | 5·533 | 5·551 |
| 0·4 | 5·369 | 5·345 | 5·396 | 5·366 | 5·376 |
| 0·5 | 5·139 | 5·151 | 5·207 | 5·165 | 5·156 |
| 0·6 | 4·903 | 4·918 | 4·963 | 4·928 | 4·894 |
| 0·7 | 4·605 | 4·629 | 4·669 | 4·636 | 4·598 |
| 0·8 | 4·304 | 4·341 | 4·346 | 4·334 | 4·277 |
| 0·9 | 3·979 | 4·016 | 3·992 | 4·000 | 3·943 |
| 1·0 | 3·656 | 3·671 | 3·629 | 3·655 | 3·604(20) |
| 1·2 | 3·037 | 3·006 | 2·958 | 2·998 | 2·956 |
| 1·4 | 2·493 | 2·383 | 2·406 | 2·415 | 2·400 |
| 1·6 | 2·041 | 1·996 | 1·993 | 2·005 | 1·964 |
| 1·8 | 1·680 | 1·694 | 1·689 | 1·689 | 1·644 |
| 2·0 | 1·408 | 1·458 | 1·450 | 1·444 | 1·412 |
| 2·2 | 1·206 | 1·266 | 1·252 | 1·248 | 1·233 |
| 2·4 | 1·053 | 1·094 | 1·084 | 1·081 | 1·081 |
| 2·6 | 0·934 | 0·945 | 0·943 | 0·942 | 0·947 |
| 2·8 | 0·836 | 0·820 | 0·826 | 0·826 | 0·828 |
| 3·0 | 0·749 | 0·727 | 0·728 | 0·732 | 0·733(10) |
| 3·5 | 0·544 | 0·545 | 0·540 | 0·543 | 0·554 |
| 4·0 | 0·405 | 0·413 | 0·413 | 0·411 | 0·425 |
| 4·5 | 0·325 | 0·325 | 0·324 | 0·325 | 0·335 |
| 5·0 | 0·263 | 0·259 | 0·259 | 0·260 | 0·273 |
| 6·0 | 0·172 | 0·173 | 0·173 | 0·173 | 0·184 |
| 7·0 | 0·120 | 0·120 | 0·120 | 0·120 | 0·128 |

ution, but the deformation is small, so justifying the use of rigid core, pseudopotential calculations (Chang & Cohen, 1984), except possibly when very accurate energy data are needed. The charge distribution of valence electrons is satisfactorily described by the Watson or Yamashita model of the oxygen ion. Comparison with the experimental isotropic Compton profiles apparently indicates that some residual basis-set deficiency affects the results here presented. To assess this point an accurate analysis of the basis-set effects on the calculated CP's is in progress; besides, new and more reliable determinations of structure factors would be extremely valuable.

## References

AIKALA, O., PAAKKARI, T. & MANNINEN, S. (1982). *Acta Cryst.* A38, 155-161.
BARRON, T. H. K. (1977). *Acta Cryst.* A33, 602-604.
BEG, M. M. (1976). *Acta Cryst.* A32, 154-156.
BERGGREN, K. F., MANNINEN, S., PAAKKARI, T., AIKALA, O. & MANSIKKA, K. S. (1977). In *Compton Scattering*, edited by B. WILLIAMS, pp. 139-208. New York: McGraw-Hill.
BURLEY, G. (1965). *J. Phys. Chem. Solids*, 26, 1605-1613.
CAUSA', M., DOVESI, R., PISANI, C. & ROETTI, C. (1986). *Phys. Rev. B*, 33, 1308-1316.

CHANG, K. J. & COHEN, M. L. (1984). *Phys. Rev. B*, **30**, 4774-4786.
DAWSON, B. (1969). *Acta Cryst.* A25, 12-29.
DOVESI, R. (1985). *Solid State Commun.* 54, 183-185.
DOVESI, R., ERMONDI, C., FERRERO, E., PISANI, C. & ROETTI, C. (1984). *Phys. Rev. B*, **29**, 3591-3600.
DOVESI, R., PISANI, C., RICCA, F., ROETTI, C. & SAUNDERS, V. R. (1984). *Phys. Rev. B*, **30**, 972-979.
DOVESI, R., PISANI, C., ROETTI, C. & SAUNDERS, V. R. (1983). *Phys. Rev. B*, **28**, 5781-5792.
GUPTA, R. K. & HARIDASAN, T. M. (1973). *Acta Cryst.* A29, 579.
LAWRENCE, J. L. (1973). *Acta Cryst.* A29, 94-95.
PATTISON, P. & WILLIAMS, B. (1976). *Solid State Commun.* 20, 585-588.
PISANI, C. & DOVESI, R. (1980). *Int. J. Quantum Chem.* 17, 501-516.

PODLOUCKY, R. & REDINGER, J. (1984). *J. Phys. C*, **16**, 6955-6969.
RACCAH, P. M. & ARNOTT, R. J. (1967). *Phys. Rev.* **153**, 1028-1031.
SANGER, P. L. (1969). *Acta Cryst.* A25, 694-702.
SCHÜLKE, W. (1977). *Phys. Status Solidi B*, **82**, 229-235.
TOGAWA, S. (1965). *J. Phys. Soc. Jpn*, **20**, 742-752.
TOGAWA, S., INKINEN, O. & MANNINEN, S. (1971). *J. Phys. Soc. Jpn*, **30**, 1132-1135.
TOKONAMI, H. (1965). *Acta Cryst.* 19, 486.
VIDAL-VALAT, G., VIDAL, J. P. & KURKI-SUONIO, K. (1978). *Acta Cryst.* A34, 594-602.
WATSON, R. E. (1958). *Phys. Rev.* **111**, 1108-1110.
WEISS, R. J. (1970). *Philos. Mag.* **21**, 1169-1173.
YAMASHITA, J. & ASANO, S. (1970). *J. Phys. Soc. Jpn*, **28**, 1143-1150.

# Neutron Diffraction Study of MgNH₄PO₄.6H₂O (Struvite) and Survey of Water Molecules Donating Short Hydrogen Bonds

BY G. FERRARIS

*Dipartimento di Scienze della Terra, Università di Torino, Via S. Massimo 22, I-10123 Torino, Italy*

AND H. FUESS AND W. JOSWIG

*Institut für Kristallographie und Mineralogie der Universität Frankfurt am Main, Senckenberganlage 30, D-6000 Frankfurt am Main 1, Federal Republic of Germany*

## Abstract

MgNH₄PO₄.6H₂O (struvite), $M_r = 245.4$, $Pmn2_1$, $a = 6.955$ (1), $b = 6.142$ (1), $c = 11.218$ (2) Å, $V = 479.2$ (2) Å³, $Z = 2$, $D_x = 1.70$ Mg m⁻³, neutrons, $\lambda = 1.179$ Å, $\mu = 0.03$ mm⁻¹, room temperature. The structure was refined from 685 unique neutron diffraction data to $R = 0.032$. The ammonium group is completely ordered and linked by one single and several polyfurcated N···O hydrogen bonds varying from 2.800 (5) to 3.498 (5) Å. Six out of eight $W$···O hydrogen bonds donated by the water molecules are in the range 2.630 (4)-2.649 (5) Å. A survey of hydrogen bonds studied by neutron diffraction reveals, on average, a linear decrease of the $W$···O bond length with Pauling bond strength ($p$) received by $W$ from coordination bonds. From the analysis of $W$···O ≤ 2.66 Å it is deduced that (i) $W$–H *vs* $W$···O correlation tends to be non-linear for short $W$···O; (ii) short $W$···O's are often connected with $W$ coordinated by $M^{n+}$ cations with $n$/(coordination number) ≥ 0.5; (iii) the experimental minimum length of 2.55 Å can be explained by the hypothesis that the bond valence of $W$–H cannot be smaller than the bond valence received by $W$ from coordination bonds.

## Introduction

The crystal structure of MgNH₄PO₄.6H₂O (struvite) was previously reported by Whitaker & Jeffery (1970a) from single-crystal X-ray data. The same authors (Whitaker & Jeffery, 1970b) reported some evidence for an ammonium group rotating around a single hydrogen bond. Ferraris & Franchini-Angela (1973) described the structure of isomorphous arsenstruvite; they proposed a disorder restricted to two mirror positions for the ammonium group. The present neutron diffraction study was performed in order to describe the hydrogen-bonding scheme completely. An accurate determination of the configuration of the water molecules in struvite is of particular interest, because these water molecules donate some of the shortest hydrogen bonds ever found in crystalline hydrates (Chiari & Ferraris, 1982; CF, hereafter).

With the aim of understanding the correlation of morphology and structure in this phase, which is present in human calculi (Abbona & Boistelle, 1979), an X-ray refinement of the struvite structure was published (Abbona, Calleri & Ivaldi, 1984) while this research was in progress.